Sang Loon Tan and Edward R.T. Tiekink*

Crystal structure of the co-crystal *N*,*N*′-bis(4-pyridylmethyl)oxalamide and 2,3,5,6-tetrafluoro-1,4-di-iodobenzene (1/1), $C_{14}H_{14}N_4O_2 \cdot C_6F_4I_2$

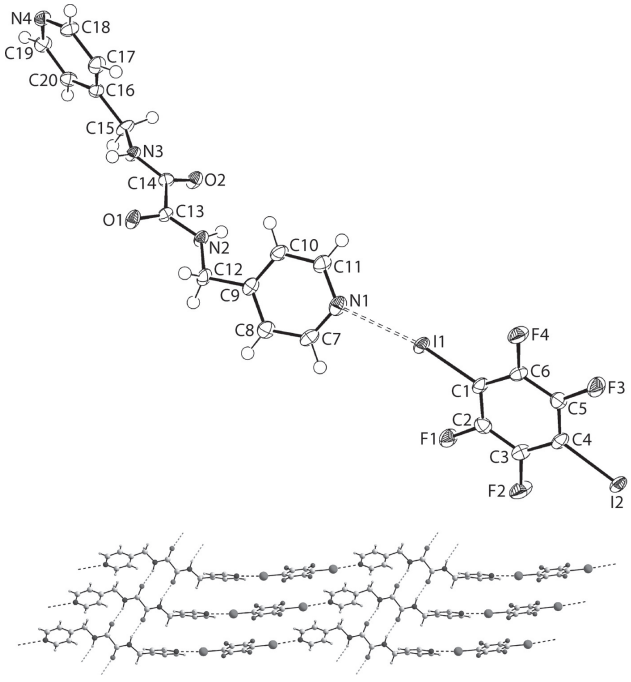

https://doi.org/10.1515/ncrs-2019-0479
Received July 9, 2019; accepted July 26, 2019; available online August 29, 2019

Abstract

$C_{20}H_{14}F_4I_2N_4O_2$, triclinic, $P\bar{1}$ (no. 2), $a = 5.0726(1)$ Å, $b = 10.9432(2)$ Å, $c = 19.8090(3)$ Å, $\alpha = 104.475(2)°$, $\beta = 90.427(2)°$, $\gamma = 92.908(2)°$, $V = 1063.10(3)$ Å^3, $Z = 2$, $R_{gt}(F) = 0.0329$, $wR_{ref}(F^2) = 0.0907$, $T = 100$ K.

CCDC no.: 1943428

The molecular structure is shown in the figure. Table 1 contains crystallographic data and Table 2 contains the list of the atoms including atomic coordinates and displacement parameters.

***Corresponding author: Edward R.T. Tiekink,** Research Centre for Crystalline Materials, School of Science and Technology, Sunway University, 47500 Bandar Sunway, Selangor Darul Ehsan, Malaysia, e-mail: edwardt@sunway.edu.my, Edward.Tiekink@gmail.com. https://orcid.org/0000-0003-1401-1520
Sang Loon Tan: Research Centre for Crystalline Materials, School of Science and Technology, Sunway University, 47500 Bandar Sunway, Selangor Darul Ehsan, Malaysia

Table 1: Data collection and handling.

Crystal:	Colourless prism
Size:	$0.18 \times 0.09 \times 0.07$ mm
Wavelength:	Cu $K\alpha$ radiation (1.54184 Å)
μ:	23.8 mm^{-1}
Diffractometer, scan mode:	XtaLAB Synergy, ω
θ_{max}, completeness:	76.6°, >99%
$N(hkl)_{measured}$, $N(hkl)_{unique}$, R_{int}:	26223, 4449, 0.054
Criterion for I_{obs}, $N(hkl)_{gt}$:	$I_{obs} > 2\,\sigma(I_{obs})$, 4243
$N(param)_{refined}$:	295
Programs:	CrysAlis^{PRO} [1], SHELX [2, 3], WinGX/ORTEP [4]

Source of material

N,*N*′-Bis(pyridin-4-ylmethyl)oxalamide, $^4LH_2$, was prepared according to the literature procedure [5] (melting point, m.pt: 474–475 K; lit. [5]: 486–487 K). 1,4-Diiodotetrafluorobenzene was purchased from Aldrich (Gillingham, Dorset, United Kingdom) and used as received without purification. The co-crystal was prepared through solvent drop-assisted grinding of $^4LH_2$ (0.154 g, 1 mmol) and 1,4-$C_6F_4I_2$ (0.402 g, 1 mmol). The mixture was ground for 15 mins in the presence of few drops of methanol that lead to a beige slurry. This was dissolved in dimethylformamide (2 mL) and carefully layered with the same volume of benzene. Colourless crystals were obtained after about three days. **M.pt**: 451–453 K. **IR** (ATR; cm^{-1}): 3282(m) ν(N—H), 3058–2938(w) ν(C—H), 1655–1642(s) ν(C=O), 1603–1511(s) ν(C=C), 1417(s) ν(C—F), 1360(m) ν(C—N), 755(s) δ(C=C), 482(s) ν(C—I).

Experimental details

The C-bound H atoms were geometrically placed (C—H = 0.95–0.99 Å) and refined as riding with $U_{iso}(H) = 1.2U_{eq}(C)$. The N-bound H-atoms were located in a difference Fourier map but were refined with a distance restraint of N—H = 0.88 ± 0.01 Å, and with $U_{iso}(H)$ set to $1.2U_{equiv}(N)$. The maximum and minimum residual electron density peaks of 2.65 and 1.59 e Å^{-3}, respectively, were located 1.00 and 0.80 Å from the I1 atom, respectively.

Table 2: Fractional atomic coordinates and isotropic or equivalent isotropic displacement parameters (Å^2).

Atom	*x*	*y*	*z*	U_{iso}*/U_{eq}
I1	−0.93660(3)	0.72803(2)	0.57419(2)	0.01511(9)
I2	−1.85947(4)	0.96049(2)	0.83098(2)	0.01554(9)
F1	−1.2374(4)	0.98419(19)	0.61693(10)	0.0229(4)
F2	−1.5833(5)	1.07247(19)	0.71513(11)	0.0257(5)
F3	−1.5620(4)	0.69523(19)	0.78998(10)	0.0231(4)
F4	−1.1973(4)	0.61157(18)	0.69594(10)	0.0215(4)
C1	−1.2092(6)	0.7939(3)	0.65246(17)	0.0148(6)
C2	−1.3121(7)	0.9113(3)	0.66020(18)	0.0170(7)
C3	−1.4939(7)	0.9564(3)	0.71006(17)	0.0164(6)
C4	−1.5862(6)	0.8858(3)	0.75486(16)	0.0153(6)
C5	−1.4846(6)	0.7679(3)	0.74753(17)	0.0158(6)
C6	−1.2971(6)	0.7243(3)	0.69823(17)	0.0150(6)
O1	0.3945(4)	0.5968(2)	0.22104(11)	0.0177(5)
O2	−0.1600(4)	0.4795(2)	0.11436(11)	0.0180(5)
N1	−0.5684(5)	0.6843(3)	0.46768(14)	0.0192(6)
N2	−0.0394(5)	0.6170(3)	0.24624(14)	0.0153(5)
H2N	−0.199(3)	0.593(3)	0.2295(19)	0.018*
N3	0.2693(5)	0.4341(2)	0.09621(13)	0.0141(5)
H3N	0.432(3)	0.449(4)	0.1126(19)	0.017*
N4	0.7928(5)	0.1093(3)	−0.07489(14)	0.0177(5)
C7	−0.4752(6)	0.7953(3)	0.45856(17)	0.0187(6)
H7	−0.540422	0.870062	0.487435	0.022*
C8	−0.2896(6)	0.8080(3)	0.40965(16)	0.0182(6)
H8	−0.227550	0.889331	0.405787	0.022*
C9	−0.1958(6)	0.6994(3)	0.36625(16)	0.0154(6)
C10	−0.2921(6)	0.5835(3)	0.37495(17)	0.0183(6)
H10	−0.233456	0.507198	0.346043	0.022*
C11	−0.4746(7)	0.5803(3)	0.42624(17)	0.0188(7)
H11	−0.536217	0.500314	0.432276	0.023*
C12	0.0081(6)	0.7098(3)	0.31267(16)	0.0176(6)
H12A	0.009152	0.795642	0.304760	0.021*
H12B	0.184608	0.698732	0.331218	0.021*
C13	0.1604(6)	0.5721(3)	0.20635(15)	0.0123(6)
C14	0.0725(6)	0.4876(3)	0.13412(15)	0.0140(6)
C15	0.2249(6)	0.3760(3)	0.02171(15)	0.0173(6)
H15A	0.224919	0.443511	−0.003513	0.021*
H15B	0.048369	0.331320	0.014776	0.021*
C16	0.4290(6)	0.2838(3)	−0.00954(16)	0.0153(6)
C17	0.5356(6)	0.2013(3)	0.02478(16)	0.0187(6)
H17	0.487556	0.203071	0.071259	0.022*
C18	0.7136(7)	0.1161(3)	−0.00964(17)	0.0178(6)
H18	0.783210	0.059389	0.014351	0.021*
C19	0.6897(7)	0.1900(3)	−0.10696(16)	0.0186(6)
H19	0.743754	0.187247	−0.153117	0.022*
C20	0.5096(6)	0.2775(3)	−0.07743(16)	0.0165(6)
H20	0.441875	0.332321	−0.102916	0.020*

Comment

As noted in a recent bibliographic review [6], isomeric molecules of the general formula (n-C_5H_4N)$CH_2N(H)C(=O)C(=O)N(H)CH_2$($C_5H_4$N-n), for n = 2, 3 and 4, hereafter abbreviated as $^nLH_2$, featured prominently in the early days of "crystal engineering." The isomeric molecules have potential hydrogen bonding functionality in the two terminal *n*-pyridyl residues (acceptors) and in the central di-amide group (donors and acceptors). Exploiting this functionality and by systematically co-crystallising $^nLH_2$ with bifunctional carboxylic acids, two-dimensional sheets could be generated. An example of this is found in the co-crystal comprising equal amounts of $^3LH_2$ and *N*,*N*′-dicarboxymethylurea [7]. The $^3LH_2$ molecules self-assembled into supramolecular tapes *via* amide-N—H···O(amide) hydrogen bonding and 10-membered amide synthons $\{\cdots HNC_2O\}_2$. Connections between parallel tapes leading to two-dimensional arrays were mediated by bifunctional carboxylic acids forming hydroxy-O—H···N(pyridyl) hydrogen bonds [7]. Using the same principles, two-dimensional sheets were generated whereby the supramolecular tapes of $^3LH_2$ formed by amide-N—H···O(amide) hydrogen bonding were linked by N···I halogen bonds, such as in the 1:1 co-crystal of $^3LH_2$ and 1,4-di-iodobuta-1,3-diyne, that is, I—C≡C—C≡C—I [8]. However, the formation of supramolecular tapes for $^nLH_2$ is not always reliable [6]. Thus, in the 1:1 co-crystal formed between $^3LH_2$ and the prototype bridging halogen-bonding molecule, 1,4-diiodotetrafluorobenzene, supramolecular tapes are formed but, mediated by *via* amide-N—H···N(pyridyl) hydrogen bonds and 18-membered $\{\cdots HNC_2NC_3N\}_2$ synthons [9]. Halogen bonding is also observed but, of the type O···I resulting in the formation of a two-dimensional array. As a part of continuing studies of the formation of multi-component crystals of $^nLH_2$ [10–12], the title 1:1 co-crystal containing the co-formers $^4LH_2$ and 1,4-diiodotetrafluorobenzene was prepared and characterised crystallographically.

The molecular structures of the independent molecules comprising the asymmetric unit, each in a general position, are shown in the figure (70% displacement ellipsoids). The central $C_2N_2O_2$ residue is approximately planar with the r.m.s. deviation of the fitted atoms being 0.0705 Å, and with the maximum deviation from the plane being 0.0948(15) Å for the O2 atom. This is in fact unusual as the central residue is usually considerably more planar [6]. The deviation from planarity arises from a twist about the central C13—C14 bond as seen in the torsion angle of O1—C13—C14—O2 of −167.6(3)°. While the C13—C14 bond length may be considered long at 1.546(4) Å, the distance falls in the usual range for $^nLH_2$ molecules, an observation ascribed to the presence of electronegative substituents at each of the carbon atoms [6]. The appended methylene-carbon atoms lie to the same side of the central plane with deviations of 0.074(5) Å, for the C12 atom, and 0.223(5) Å, for C15. The pyridyl rings also lie to the same side of the molecule so that the conformation approximates syn-periplanar. The dihedral angle between the central plane

and the N1- and N4-pyridyl rings are 68.32(10) and 63.82(9)°, respectively. The dihedral angle between the pyridyl rings is 47.90(11)°, consistent with a splayed relationship, and emphasises the conformational flexibility of these molecules [6]. As is always observed in the $^{n}LH_2$ molecules [6], intramolecular amide-N—H···O(amide) hydrogen bonds are evident which give rise to *S*(5) loops [N2—H2n···O2: H2n···O2 = 2.32(4) Å, N2···O2 = 2.717(3) Å with angle at H2n = 107(2)° and N3—H3n···O1: H3n···O1 = 2.36(4) Å, N3···O1 = 2.711(3) Å with angle at H3n = 104(2)°].

As evident from the figure, the independent molecules are connected by N···I halogen bonds [N1···I1 = 2.795(3) Å and, from symmetry, $N4\cdots I2^{i} = 2.840(3)$ Å for symmetry operation (i) 3 + x, −1 + y, −1 + z]. The result is a linear supramolecular chain along [3 −1 −1]. Links between chains leading to a two-dimensional array are of the type amide-N—H···O(amide) hydrogen bonding and as these occur on either side of the central di-amide residue, a supramolecular tape is sustained by these interactions [N2—H2n···$O1^{ii}$: H2n···$O1^{ii}$ = 2.071(16) Å, N2···$O1^{ii}$ = 2.899(3) Å with angle at H2n = 158(3)°; N3—H3n···$O2^{iii}$: H3n···$O2^{iii}$ = 2.078(17) Å, N3···$O2^{iii}$ = 2.917(3) Å with angle at H3n = 160(3)° for (ii) −1 + x, y, z and (iii) 1 + x, y, z]. The aforementioned layers are connected into double-layers via methylene-C—H···O(amide) interactions [C15—H15a···$O2^{iv}$: H15a···$O2^{iv}$ = 2.57 Å, C15···$O2^{iv}$ = 3.471(4) Å with angle at H15a = 152° for (iv) −x, 1−y, −z]. The double layers interdigitate so that fluoro atoms lie in voids defined by the 1,4-diiodotetrafluorobenzene molecules but, directional interactions are not apparent. Accordingly, in order to understand more about the supramolecular interactions stabilising the crystal, the structure was further evaluated using Crystal Explorer 17 [13] to calculate the Hirshfeld surfaces along with the full and delineated fingerprint plots guided by established procedures [14]. The analysis of the calculated Hirshfeld surface for the complete asymmetric unit of the title structure revealed a myriad of different types of contacts with the most prevalent being F···H/H···F at 26.2% but, at separations greater than the sum of the van der Waals radii. Other major contributors to the contacts were found to be H···H [14.1%], C···H/H···C [13.4%], O···H/H···O [9.3%], I···C/C···I [9.1%] and I···H/H···I [7.6%], with only the H···O contacts being less than the sum of the respective van der Waals radii; I···N/N···I interactions only amounted to 3.1% of all surface contacts.

The calculations were also performed on the individual co-crystal co-formers. For $^{4}LH_2$, reflecting the composition of the molecule, the percentage contributions from H···H [21.7%], C···H/H···C [17.3%] and O···H/H···O [14.7%] contacts all increased in significance while F···H/H···F [19.9%], I···C/C···I [2.7%] and [I···H/H···I [5.0%] decreased. As expected, the opposite trends in surface contacts are evident for the 1,4-diiodotetrafluorobenzene molecule with diminished contributions from H···H [0.0%], C···H/H···C [5.4%] and O···H/H···O [0.0%] contacts but, significantly increased contributions from F···H/H···F [33.3%], I···C/C···I [18.6%] and [I···H/H···I [16.2%] contacts to the calculated surface.

Acknowledgements: Sunway University Sdn Bhd is thanked for financial support of this work through Grant no. STR-RCTR-RCCM-001-2019.

References

1. Rigaku Oxford Diffraction: CrysAlis^{PRO}. Rigaku Oxford Diffraction Ltd, Yarnton, England (2017).
2. Sheldrick, G. M.: A short history of SHELX. Acta Crystallogr. **A64** (2008) 112–122.
3. Sheldrick, G. M.: Crystal structure refinement with SHELXL. Acta Crystallogr. **C71** (2015) 3–8.
4. Farrugia, L. J.: WinGX and ORTEP for Windows: an update. J. Appl. Crystallogr. **45** (2012) 849–854.
5. Nguyen, T. L.; Scott, A.; Dinkelmeyer, B.; Fowler, F. W.; Lauher, J. W.: Design of molecular solids: utility of the hydroxyl functionality as a predictable design element. New J. Chem. **22** (1998) 129–135.
6. Tiekink, E. R. T.: Multi-component crystals: synthesis, concepts, function. (Ed. Tiekink E. R. T. and Schpector-Zukerman J.), p. 289–319. De Gruyter, Singapore (2017).
7. Nguyen, T. L.; Fowler, F. W.; Lauher, J. W.: Commensurate and incommensurate hydrogen bonds. an exercise in crystal engineering. J. Am. Chem. Soc. **123** (2001) 11057–11064.
8. Goroff, N. S.; Curtis, S. M.; Webb, J. A.; Fowler, F. W.; Lauher, J. W.: Designed cocrystals based on the pyridine-iodoalkyne halogen bond. Org. Lett. **7** (2005) 1891–1893.
9. Hursthouse M. B.; Gelbrich, T.; Plater M. J.: Private communication to the Cambridge Structural Database. Z. Kristallogr. NCS (2003).
10. Tan, S. L.; Tiekink, E. R. T.: *N*,*N*′-bis(4-Pyridylmethyl)oxalamide benzene solvate: crystal structure, Hirshfeld surface analysis and computational study. Acta Crystallogr. **E75** (2019) 1133–1139.
11. Tan, S. L.; Tiekink, E. R. T.: Crystal structure of the 1:2 co-crystal between *N*,*N*′-bis(4-pyridylmethyl)oxalamide and acetic acid as a dihydrate, $C_{14}H_{14}N_4O_2{\cdot}2\,C_2H_4O_2{\cdot}2\,H_2O$. Z. Kristallogr. NCS **234** (2019) 1109–1111.
12. Tan, S. L.; Tiekink, E. R. T.: Crystal structure of the co-crystal *N*,*N*′-bis(3-pyridylmethyl)oxalamide acetic acid (1/2), $C_{14}H_{14}N_4O_2{\cdot}2C_2H_4O_2$. Z. Kristallogr. NCS **234** (2019) 1113–1116.
13. Turner, M. J.; Mckinnon, J. J.; Wolff, S. K.; Grimwood, D. J.; Spackman, P. R.; Jayatilaka, D.; Spackman, M. A.: Crystal Explorer v17. The University of Western Australia, Australia (2017).
14. Tan, S. L.; Jotani, M. M.; Tiekink, E. R. T.: Utilizing Hirshfeld surface calculations, non-covalent interaction (NCI) plots and the calculation of interaction energies in the analysis of molecular packing. Acta Crystallogr. **E75** (2019) 308–318.